



# Synergistic effects of heterotrophic and phototrophic metabolism for *Haematococcus lacustris* grown under mixotrophic conditions

Lars Stegemüller<sup>1</sup> · Borja Valverde-Pérez<sup>2</sup> · Anders Thygesen<sup>1</sup> · Irimi Angelidaki<sup>1</sup>

Received: 16 February 2024 / Revised: 17 July 2024 / Accepted: 19 July 2024  
© The Author(s) 2024

## Abstract

Mixotrophic cultivation of *Haematococcus lacustris* is one of the most promising strategies to produce natural astaxanthin. During mixotrophic growth, microalgae assimilate and metabolize organic carbon in addition to photosynthetic growth, resulting in increased biomass productivity. Several studies have evaluated the effect of different organic carbon sources on mixotrophic growth in various microalgae species. However, knowledge of detailed growth kinetics as a function of substrate concentration and light intensity is lacking. In this study, the growth kinetics of *H. lacustris* using four different carbon sources and the effect of light under mixotrophic and photoautotrophic conditions are described. Mixotrophic cultivation showed significant differences in respect to applied substrate and achieved maximum specific growth rates of  $0.91 \pm 0.13$ ,  $0.19 \pm 0.05$ ,  $0.36 \pm 0.05$ , and  $0.23 \pm 0.05$  day<sup>-1</sup>, for acetate, methanol, glucose, and glycerol, respectively. Optimal growth at mixotrophic conditions using acetate was 1.8 times higher than the sum of hetero- and photoautotrophic growth. Furthermore, the optimum light intensity was 1.3 times higher for mixotrophic than for autotrophic growth. Thus, mixotrophy increases light intensity tolerance. These results indicate a strong interconnection between carbon metabolism and photosynthetic activity and lay the foundation for more detailed mathematical models describing the mixotrophic growth of *H. lacustris*.

**Keywords** Microalgae · Chlorophyceae · Light intensity · Acetate · Glucose · Glycerol · Methanol

## Introduction

Microalgae are known for their high nutritional value, including proteins, carbohydrates, lipids, and pigments like astaxanthin or  $\beta$ -carotene (Lam et al. 2018). They can grow with high areal productivities (estimated values range between 34 and 61 t ha<sup>-1</sup> year<sup>-1</sup>) by using sunlight to convert CO<sub>2</sub> into biomass, via photoautotrophic growth (Ruiz et al. 2016). Moreover, some microalgae species can grow mixo- and heterotrophically, which means they can utilize organic carbon sources (e.g., acetate or glucose) in addition to CO<sub>2</sub> with (mixotrophy) or without (heterotrophy) light as an energy source (Vidotti et al. 2020).

One particularly interesting microalgae is *Haematococcus lacustris* (formerly known as *Haematococcus pluvialis*), a flagellated green freshwater microalgae (Han et al., 2004). The cell cycle of *H. lacustris* is complex. Depending on the environment (e.g., light intensity, nutrient availability, temperature) the cell undergoes morphological and physiological changes accompanied by biochemical alterations (Zhang et al. 2017). One of the most prominent cell cycle observations is the transition from green to red cells and vice versa. Red cells are rich in astaxanthin which is a bright red secondary carotenoid with health-promoting properties for humans and animals. Among the positive effects of astaxanthin, are antioxidant and anti-inflammatory effects (Ambati et al. 2014). Given the high content of astaxanthin (up to 4% dry weight), *H. lacustris* is considered the best natural source of astaxanthin (Ranga Rao et al. 2010). Most commonly, a two-stage cultivation strategy is applied where *H. lacustris* is first grown under favorable conditions, followed by an induction phase to increase the content of astaxanthin (Li et al. 2020). However, *H. lacustris* grows relatively slowly and therefore supplementation of organic carbon sources, which can significantly increase microalgae biomass productivities,

✉ Lars Stegemüller  
lsest@dtu.dk

<sup>1</sup> Department of Chemical Engineering, Technical University of Denmark, DTU, Søtofts Plads 228A, 2800 Lyngby, Denmark

<sup>2</sup> Department of Environmental and Resource Engineering, Technical University of Denmark, DTU, Bygningstorvet 115, 2800 Lyngby, Denmark

could improve the growth phase (Abreu et al. 2022; Yu et al. 2022a). In practice, heterotrophic cultivation poses major challenges such as low astaxanthin content and lower growth rates compared to photoautotrophic growth (Zhang et al. 2016; Proietti Tocca et al. 2024). Therefore, mixotrophic growth could be a viable solution to improve the biotechnological production of astaxanthin from *H. lacustris*.

Commonly, chemically defined media are used for cultivation, which are expensive. Therefore, the utilization of wastewater and industrial side streams is receiving increasing interest as it can result in a win–win situation. In the best case, a low-cost substrate is valorized while at the same time costs for treatment or disposal are avoided. These side streams are often rich in organic carbon, nitrogen, and phosphorous, which microalgae can take up efficiently and convert into valuable products such as antioxidants (Pan et al. 2021). However, depending on the intended use of the grown biomass, not all waste streams are suitable. A thoughtful selection with a focus on required pretreatments, contaminations, pH range and more is therefore inevitable (Maurya et al. 2022). Some suitable waste streams could be obtained from anaerobic processes, biodiesel production, and kraft pulping mills, rich in acetate, glycerol, and methanol, respectively (Lin et al. 2008; Pan et al. 2017; Mohamadia et al. 2023).

Understanding the carbon metabolism of *H. lacustris* is essential to adapt and optimize production processes. When light and organic carbon are provided simultaneously, a synergistic effect related to CO<sub>2</sub> and O<sub>2</sub> availability can be observed. The activity of both metabolic pathways results in higher local CO<sub>2</sub> and O<sub>2</sub> concentration which leads to higher activity of the Calvin and the tricarboxylic acid cycle (TCA cycle), respectively (Smith et al. 2015). Although there are many reports about the use of several organic carbon substrates for mixotrophic growth of *H. lacustris*, the exact mechanisms behind the carbon metabolism in *H. lacustris* are often not completely understood yet (Abreu et al. 2022). However, through studies of other microalgae species and plants, a small overview of the metabolic pathways and uptake mechanisms can be drawn. In the following, the focus is put on acetate, glucose, glycerol, and methanol since they could be cost-effective residual sources or industrial byproducts and are at the same time bioavailable for *H. lacustris*. Glucose is among the most used substrates in biotechnological processes and can be taken up by *H. lacustris* through active transporters (Sauer and Tanner 1989). Glucose-6-phosphate is then readily available for storage, cell synthesis, and respiration (Perez-Garcia et al. 2011). The monocarboxylic/proton transporter is responsible for the uptake of acetate. Once acetate enters the cell, coenzyme A reacts with the acetate to form acetyl-CoA (Droop 1974; Becker et al. 2005). Microalgae growing on acetate must have the glyoxylate cycle, which shares several metabolites

with the TCA cycle. Therefore, the carbon originating from acetate can ultimately enter the TCA cycle and be assimilated in the form of carbon skeletons or produce adenosine triphosphate (ATP) in the mitochondria (Neilson and Lewin 1974; Boyle and Morgan 2009). Both glycerol and methanol do not require any active transport, since they can enter the cell by diffusion (Neilson and Lewin 1974; Cooper and Hausman 2013). Several species can metabolize glycerol in the presence of light. However, growth appeared to be inhibited under dark conditions (Ingram et al. 1973; Kaplan et al. 1986; Dechatiwongse and Choorit 2021). Similarly, the growth-enhancing effects of methanol on microalgae are stronger during illumination (Choi et al. 2011). The proposed pathway for methanol assimilation is the conversion of methanol to CO<sub>2</sub> (Kotzabasis et al. 1999).

Currently, there are no detailed kinetic studies for mixotrophic growth in *H. lacustris* describing both the growth kinetics on the individual carbon sources as well as the interaction at different light intensities. The integration of theoretical knowledge with quantitative experimental data will unlock novel avenues for the implementation of mixotrophic growth in industrial processes. This study gives a detailed description of mixotrophic growth kinetics in *H. lacustris* for four relevant carbon sources from potential residual streams. Substrate concentration as well as the influence of light under mixo- and photoautotrophic conditions were investigated to identify optimal growth conditions and enable accurate mathematical model descriptions.

## Materials and methods

### Microalgal cultures

The strain *Haematococcus lacustris* SAG 192.80 was obtained from the culture collection of algae at Goettingen University. Pre-cultures were maintained in 250 mL shake flasks with 100 mL of culture and periodically examined with field microscopy using a VisiScope TL534B-SA FL4 microscope (VWR, USA; SI). The incubator was set to 25 °C, 150 rpm, 12/12 day/night cycle and 39 μmol photons m<sup>-2</sup> s<sup>-1</sup> white light. Day/night cycles at a low light intensity were used as they are reported to be optimal for the growth of vegetative green cells of *H. lacustris* (Domínguez et al. 2019; Oslan et al. 2021). All cultures were grown in MES Volvox medium (Starr and Zeikus 1993), modified by adding 5 g L<sup>-1</sup> HEPES buffer and the respective carbon sources glucose, sodium acetate, methanol and glycerol. The pH was adjusted to 6.7 using 1 M sodium hydroxide and never exceeded 7.1 during any experiment.

Microplate experiments were conducted in 24-well microtiter plates (BioLite 24 Well Multidish, Thermo Scientific) with 2 mL medium per well. The microplates were placed in

the same environment as the pre-cultures. Pre-cultures were centrifuged ( $2415 \times g$ , 5 min) and the cell pellet was suspended in MES Volvox medium with  $5 \text{ g L}^{-1}$  HEPES buffer. The respective carbon source was added at concentrations of 0.5, 1, 2.5, 5, 10, 20, 30 and 40 mM carbon (mM C). To monitor the growth along with the uptake, three wells were sampled at every second measuring point (starting from 12 replicates at  $t_0$ ) and the concentration of the respective carbon source was measured (Wagner et al. 2016).

The effect of light intensity on the photoautotrophic and mixotrophic growth with  $1 \text{ g L}^{-1}$  sodium acetate was investigated with neutral density filters mounted 1 cm above the microplate. Nine different incident light intensities in a range from 7.4 to  $55 \mu\text{mol photons m}^{-2} \text{ s}^{-1}$  were applied. Within this range both light limitation and light saturation could be observed.

Batch experiments in heterotrophic conditions were performed with  $1 \text{ g L}^{-1}$  sodium acetate as the carbon source using 250 mL glass bottles. The bottles were completely covered with black foil and placed in the same incubator as the pre-culture and microplates. Additionally, the bottles were aerated with filter-sterilized (pore size  $0.2 \mu\text{m}$ ; Sartorius, Germany) ambient air to avoid oxygen limitation.

## Analytical methods

The light intensities received by the wells were measured at the height of the microplate by a mobile light sensor (LI-190SA  $2 \pi$  quantum sensor, Li-Cor, USA). Growth in the microplate experiments was monitored through *in-vivo* fluorescence (IVF) at 440 nm excitation and 690 nm emission using a BIOTEK Synergy microplate reader (Van Wagenen et al. 2014). IVF measurements are less susceptible to bacterial contamination than optical density measurements due to the direct correlation with microalgae pigmentation. Biomass in the batch experiments was measured through the optical density (OD) at 750 nm. Both measurements were linearly correlated to total suspended solids (TSS; Online Resource 5). TSS were obtained based on the APHA 2540-D standard method using glass fiber filters with a pore size of  $0.7 \mu\text{m}$  (Whatman GF/F, UK; (APHA 1999)). Acetate and methanol concentrations were determined by gas chromatography (GC; Agilent 7890A equipped with a SGE capillary  $30 \text{ m} \times 0.53$  with  $1 \mu\text{m}$  film column) analysis. The oven was programmed to hold  $45 \text{ }^\circ\text{C}$  for 3.5 min before ramping up the temperature to  $210 \text{ }^\circ\text{C}$  in steps of  $15 \text{ }^\circ\text{C min}^{-1}$  and the final temperature was held for 4 min. Prior to the analyses, 1.5 mL sample was acidified with  $100 \mu\text{L}$  34% v/v *ortho*- $\text{H}_3\text{PO}_4$ . After centrifugation (12,000 rpm, 7 min), 1 mL supernatant was transferred to the GC vial and  $100 \mu\text{L}$  internal standard of  $500 \text{ mg L}^{-1}$  4-methylvaleric acid was added to the vial.

Glucose and glycerol were measured by Dionex ICS-6000 DC as described in Vigato et al. (2022).

## Data analysis

A one-way ANOVA analysis followed by Fisher's least significant difference test (LSD,  $p < 0.05$ ) was conducted to validate significant differences in the growth rates at the different substrate concentrations. Homogeneity and normality of the data were confirmed prior to the ANOVA analysis using Levene's test ( $p = 0.05$ ) and Q-Q plots, respectively. The statistical analyses and computation of the mathematical functions were performed using Origin-Pro 2021 and MATLAB R2021b (OriginLab Corporation, USA and Mathworks, USA), respectively.

Growth rates ( $\mu$ ,  $\text{day}^{-1}$ ) and yields ( $Y_{x/s}$ ,  $\text{g-TSS g-substrate}^{-1}$ ) were calculated during the exponential growth phase at low cell densities ranging from 0.05 and  $0.15 \text{ g L}^{-1}$ :

$$\mu = \ln\left(\frac{C_{x2}}{C_{x1}}\right)/(t_2 - t_1) \quad (1)$$

$$Y_{x/s} = \frac{C_{x2} - C_{x1}}{C_{s1} - C_{s2}} \quad (2)$$

where,  $C_x$  and  $C_s$  are the concentration of TSS and the respective substrate ( $\text{g L}^{-1}$ ); 1 and 2 denote the time ( $t$ ,  $\text{day}^{-1}$ ).

The specific light intensity  $I$  ( $\mu\text{mol mg}_x^{-1} \text{ m}^{-2} \text{ s}^{-1}$ ) was calculated for a better comparison of the different batches, since the biomass concentration varied from 0.05 to  $0.15 \text{ g L}^{-1}$ . The average biomass concentration  $C_{x,av}$  ( $\text{g L}^{-1}$ ) between the time points used to compute the growth rates was utilized. The volume  $V_m$  was 2 mL in all batches.

$$I = \frac{I_{in}}{V_m \cdot C_{x,av}} \quad (3)$$

Error propagation was used to calculate the error of the growth rates and yields, as follows:

$$\frac{\sigma_\mu}{\mu} = \sqrt{\left(\frac{\sigma_{t1}}{C_{x1}}\right)^2 + \left(\frac{\sigma_{t2}}{C_{x2}}\right)^2} \quad (4)$$

$$\frac{\sigma_Y}{Y} = \sqrt{\left(\frac{\sigma_{C_x}}{C_x}\right)^2 + \left(\frac{\sigma_{C_s}}{C_s}\right)^2} \quad (5)$$

where,  $\mu$  and  $Y$  are the result of function (1) and \\*MERGEFORMAT (2), respectively;  $C_x$  and  $C_s$  are the average measurements and  $\sigma$  is the respective standard deviation.

The root mean squared normalized error (RMSNE) was determined to give an indication of the accuracy of the model predictions:

$$RMSNE = \sqrt{\frac{1}{n} \sum_{i=1}^n \left( \frac{y_m - y}{y_m} \right)^2} \quad (6)$$

where,  $n$  is the number of measurement points,  $y_m$  is the observed value and  $y$  is the predicted value.

## Model overview

Different kinetic models were tested to illustrate the dependency between substrate concentration, light intensity and growth rate (Table 1). The MATLAB function *lsqcurvefit* was applied to fit the model equations to empirical data and obtain the model parameters.

The Monod equation models the growth rate of microorganisms as a function of substrate concentration, the growth rate approaches 0 when the substrate concentration is 0 (Monod 1949). However, *H. lacustris* can grow in the absence of organic substrate as long light is available. This required the introduction of an additional parameter  $p$ , which corrects for phototrophic growth and prevents the function from approaching 0 in the absence of organic substrate.

Similarly, the Steele function, which describes the relationship between growth rate and light intensity, is zero at the origin (Steele 1962). It was expanded to account for the compensation light intensity  $I_{ph,c}$ , which is defined as the irradiance above which the growth rate is positive (Barbera et al. 2015). This enabled the model to have a non-zero intersection at zero growth and therefore depict the light energy required for cellular maintenance.

## Results

### Mixotrophic growth on different carbon sources

The effect of organic carbon in mixotrophic growth of *H. lacustris* was investigated at different initial carbon

concentrations and monitored by in-vivo fluorescence. To determine the mixotrophic growth kinetics the cultures were grown at different carbon concentrations in microplates. In addition, a data fit is presented to underline the observed kinetic behavior. Mixotrophic cultures with glucose (Fig. 1a), methanol (Fig. 1b), glycerol (Fig. 1c), and acetate (Fig. 1d) achieved a maximum specific growth rate of  $0.36 \pm 0.05$ ,  $0.19 \pm 0.05$ ,  $0.23 \pm 0.05$ , and  $0.91 \pm 0.13 \text{ d}^{-1}$  at 40, 10, 10 and 1 mM C, respectively. Mixotrophic growth on acetate followed zero-order kinetics, without observing a significant influence of substrate concentration on growth rates (ANOVA:  $F(8,7)=0.55$ ,  $p=0.79$ ). Glucose, glycerol, and methanol cultures exhibited significantly different growth behavior depending on the substrate concentration. Cultures grown on glucose and methanol can be described by an adapted Monod equation ( $R^2=0.92$  and  $0.79$ ), accounting for photoautotrophic growth when no substrate is added. Only glycerol cultures experienced substrate inhibition above 20 mM C in the presented study and was therefore described by the Haldane/Andrews model. Additionally, a photoautotrophic control cultivation was performed, resulting in a growth rate of  $0.23 \pm 0.02 \text{ day}^{-1}$ . An overview of the determined kinetic parameters and performance indices of the models are presented in Table 2.

To validate the biochemical conversion of the substrates, the carbon sources were monitored (Table 3). Uptake and conversion of sodium acetate, glucose, and methanol were confirmed, while glycerol uptake could not be confirmed, since no significant difference was detected through ICS analysis. The highest yield of TSS on substrate was 0.563 and 0.449  $\text{g g}^{-1}$  observed at 10 mM C using sodium acetate and glucose, respectively. It should be noted that the yield of TSS on substrate does not depict the total efficiency of assimilated carbon which is converted to biomass since the fixation of  $\text{CO}_2$  also contributes to biomass. However, the yield gives an indication of the efficiency to which the supplemented organic carbon contributes toward growth.

**Table 1** Overview of the applied models including the associated equations and parameters

Model	Equation	Parameters	Citation
Adapted from Monod	$\mu = p + \mu_{max} \cdot \frac{S}{S+K_S}$	$\mu$ : specific growth rate [ $\text{day}^{-1}$ ] $\mu_{max}$ : maximum specific growth rate on substrate [ $\text{day}^{-1}$ ] $S$ : substrate concentration [mM C] $K_S$ : half-saturation constant [mM C] $p$ : regression parameter associated with photoautotrophic growth [ $\text{day}^{-1}$ ]	(Monod 1949)
Adapted Steele	$\mu = \mu_{max} \cdot \frac{I - I_{ph,c}}{I_{max} - I_{ph,c}} \cdot e^{-\frac{I - I_{ph,c}}{I_{max} - I_{ph,c}}}$	$I$ : specific light intensity [ $\mu\text{mol}_{ph} \text{ mg}_x^{-1} \text{ m}^{-2} \text{ s}^{-1}$ ] $I_{max}$ : optimum light intensity [ $\mu\text{mol}_{ph} \text{ mg}_x^{-1} \text{ m}^{-2} \text{ s}^{-1}$ ] $I_{ph,c}$ : compensation light intensity [ $\mu\text{mol}_{ph} \text{ mg}_x^{-1} \text{ m}^{-2} \text{ s}^{-1}$ ]	(Steele 1962)
Haldane / Andrews	$\mu = \mu_{max} \cdot \frac{S}{S + \left( \frac{S^2}{K_I + K_S} \right)}$	$K_I$ : inhibition constant [mM C]	(Haldane 1930; Andrews 1968)

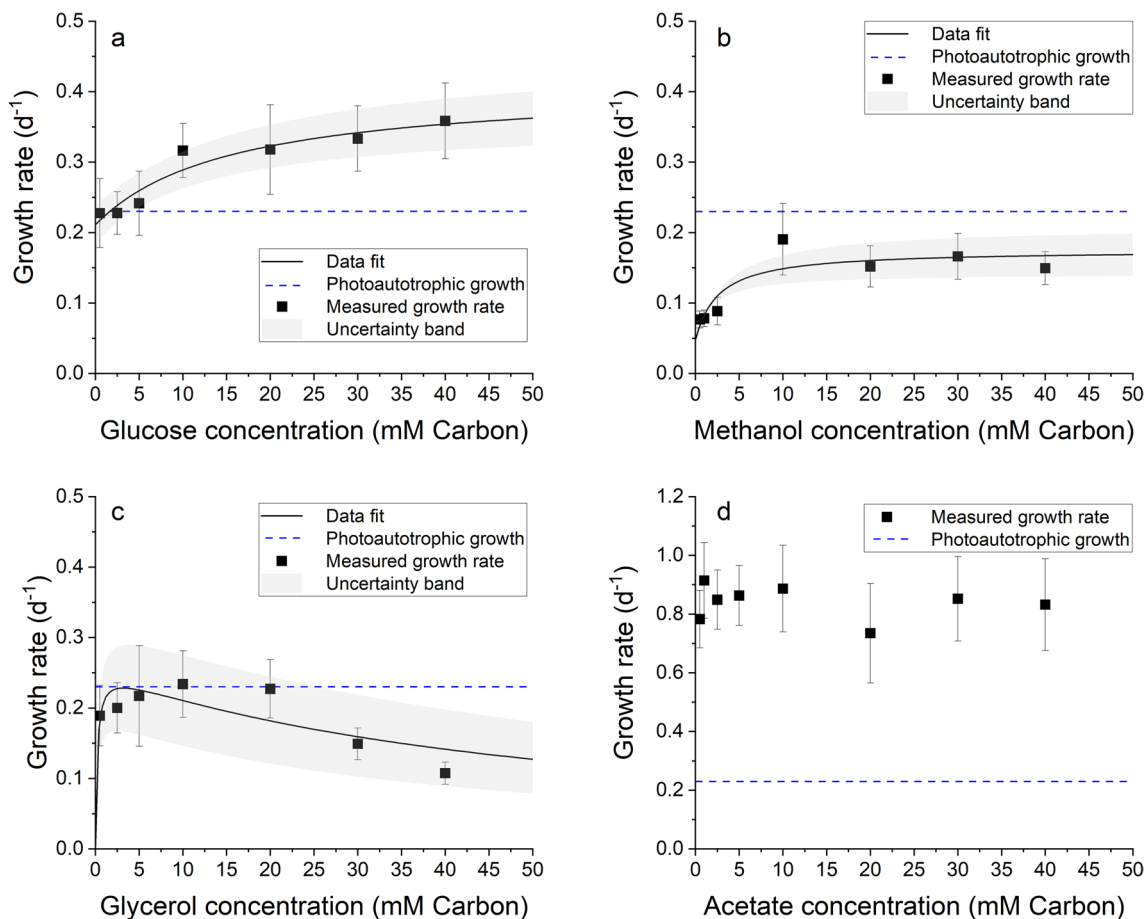


**Fig. 1** Calculated growth rates of *H. lacustris* grown mixotrophically with glucose (**a**), methanol (**b**), glycerol (**c**) and acetate (**d**) as a function of the substrate concentration at a light intensity of  $39 \mu\text{mol photons m}^{-2} \text{s}^{-1}$ . Note that the y-axis of plot d is scaled differently. Error

bars indicate the standard deviation from  $n \geq 6$  biological replicates (see SI). The grey bands show the uncertainty based on the RMSNE of the model parameters

**Table 2** Overview of kinetic parameters with standard error and performance indices of the applied model formulations. The coefficient of determination  $R^2$  and the root mean squared normalized error (RMSNE) are presented as performance indices

Substrate	Applied model	Kinetic parameters	$R^2$ (-)	RMSNE
Glucose	Modified Monod	$\mu_{max} = 0.198 \pm 0.027 \text{ day}^{-1}$ $K_S = 15.410 \pm 3.470 \text{ mM C}$ $p = 0.211 \pm 0.026 \text{ d}^{-1}$	0.92	0.014
Methanol	Modified Monod	$\mu_{max} = 0.128 \pm 0.033 \text{ day}^{-1}$ $K_S = 2.609 \pm 0.814 \text{ mM C}$ $p = 0.047 \pm 0.000 \text{ day}^{-1}$	0.79	0.020
Glycerol	Haldane / Andrews	$\mu_{max} = 0.258 \pm 0.067 \text{ day}^{-1}$ $K_S = 0.206 \pm 0.031 \text{ mM C}$ $K_I = 48.840 \pm 13.565 \text{ mM C}$	0.62	0.026
Acetate	None	Zero order kinetics	-	-

## Influence of light intensity

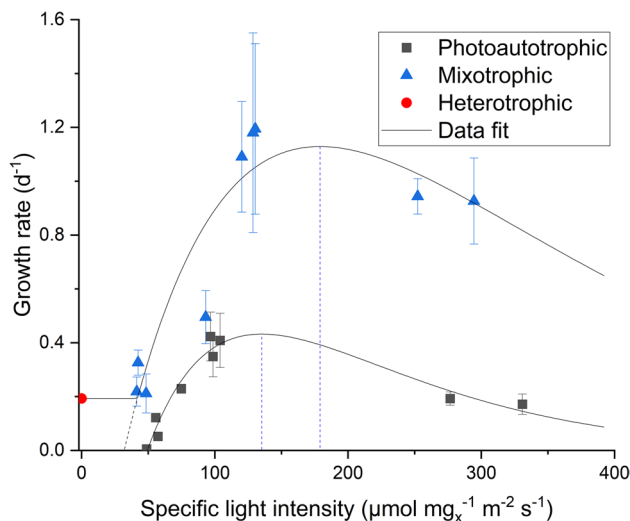
The effect of the light intensity on the growth of *H. lacustris* under photoautotrophic and mixotrophic conditions was investigated at nine different specific light intensities with sodium acetate being supplemented during the mixotrophic

cultivation. To reduce effects of self-shading, the cultivations were performed at low cell densities between  $0.05$  and  $0.15 \text{ g L}^{-1}$  and the light intensities were normalized to specific light intensity per mg of biomass. The Steele expression was adapted to include a compensation point of photoautotrophic growth ( $I_{ph,c}$ ), at which the light intensity



**Table 3** Growth rates and yields with the respective carbon source at different concentrations at a light intensity of 39  $\mu\text{mol photons m}^{-2} \text{s}^{-1}$ . The yields are displayed as g-TSS per g-substrate. Yields aregiven with the respective standard deviation of  $n=3$  biological replicates. Literature values marked with a star were recalculated to match the units used in this study

Concentration (mM C)	Acetate		Glucose		Methanol		Glycerol
	Growth rate ( $\text{day}^{-1}$ )	TSS Yield ( $\text{g g}^{-1}$ )	Growth rate ( $\text{day}^{-1}$ )	TSS Yield ( $\text{g g}^{-1}$ )	Growth rate ( $\text{day}^{-1}$ )	TSS Yield ( $\text{g g}^{-1}$ )	Growth rate ( $\text{day}^{-1}$ )
10	$0.89 \pm 0.15$	$0.56 \pm 0.04$	$0.32 \pm 0.10$	$0.45 \pm 0.01$	$0.19 \pm 0.05$	$0.27 \pm 0.18$	$0.23 \pm 0.05$
20	$0.74 \pm 0.17$	$0.26 \pm 0.04$	$0.32 \pm 0.10$	$0.21 \pm 0.06$	$0.15 \pm 0.03$	$0.32 \pm 0.25$	$0.23 \pm 0.04$
30	$0.85 \pm 0.14$	$0.32 \pm 0.03$	$0.33 \pm 0.11$	$0.25 \pm 0.05$	$0.17 \pm 0.03$	$0.16 \pm 0.09$	$0.15 \pm 0.02$
40	$0.83 \pm 0.16$	$0.20 \pm 0.03$	$0.36 \pm 0.14$	$0.40 \pm 0.06$	$0.15 \pm 0.02$	$0.15 \pm 0.05$	$0.11 \pm 0.02$
163*	Incremental increase of light intensity from 60 to 170 $\mu\text{mol photons m}^{-2} \text{s}^{-1}$ (Oncel et al. 2011)						0.47
65.2*	250 $\mu\text{mol photons m}^{-2} \text{s}^{-1}$ light intensity with 8/16 day/night cycle (Andruleviciute et al. 2014)						$0.22 \pm 0.03$
326.1*							$0.31 \pm 0.03$
166.66*			0.60	Incremental increase of light intensity from 60 to 170 $\mu\text{mol photons m}^{-2} \text{s}^{-1}$ (Oncel et al. 2011)			
15*	0.57			250 $\mu\text{mol m}^{-2} \text{s}^{-1}$ light intensity with 12/12 day/night cycle (Kobayashi et al. 1992)			
45*	0.60	1.08*					
60*	0.59						

**Fig. 2** Light-growth dependency of mixo- and photoautotrophic cultivations of *H. lacustris*. Heterotrophic growth was observed independently of the other experiments. The dashed line indicates the continuation of the model prediction using the Steele expression as well as the respective maxima of the function. Error bars indicate the standard deviation of  $n=4$  biological replicates

is just sufficient for the cell to produce enough sugar to keep the cellular maintenance up. A comparison between the adapted Steele expression and the original Steele expression is shown in supplementary information. Accounting for this, the expression describes the obtained data most accurately, resulting in an  $R^2$  of 0.95 and 0.86 for photoautotrophic and mixotrophic growth, respectively (Fig. 2). The estimated values for  $\mu_{max}$ ,  $I_{max}$  and  $I_{ph,c}$  for photoautotrophic and mixotrophic growth were  $0.43 \pm 0.09$  and  $1.13 \pm 0.23 \text{ day}^{-1}$ ,

$135.31 \pm 0.53$  and  $179.02 \pm 16.84 \mu\text{mol}_{ph} \text{mg}_x^{-1} \text{m}^{-2} \text{s}^{-1}$ ,  $49.31 \pm 0.87$  and  $31.98 \pm 1.26 \mu\text{mol}_{ph} \text{mg}_x^{-1} \text{m}^{-2} \text{s}^{-1}$ , respectively. Heterotrophic cultivation with sodium acetate was performed in 250 mL flasks to display the actual growth rate in dark conditions, resulting in an observed growth rate of  $0.19 \pm 0.01 \text{ day}^{-1}$ .

## Discussion

### Mixotrophic growth on different carbon sources

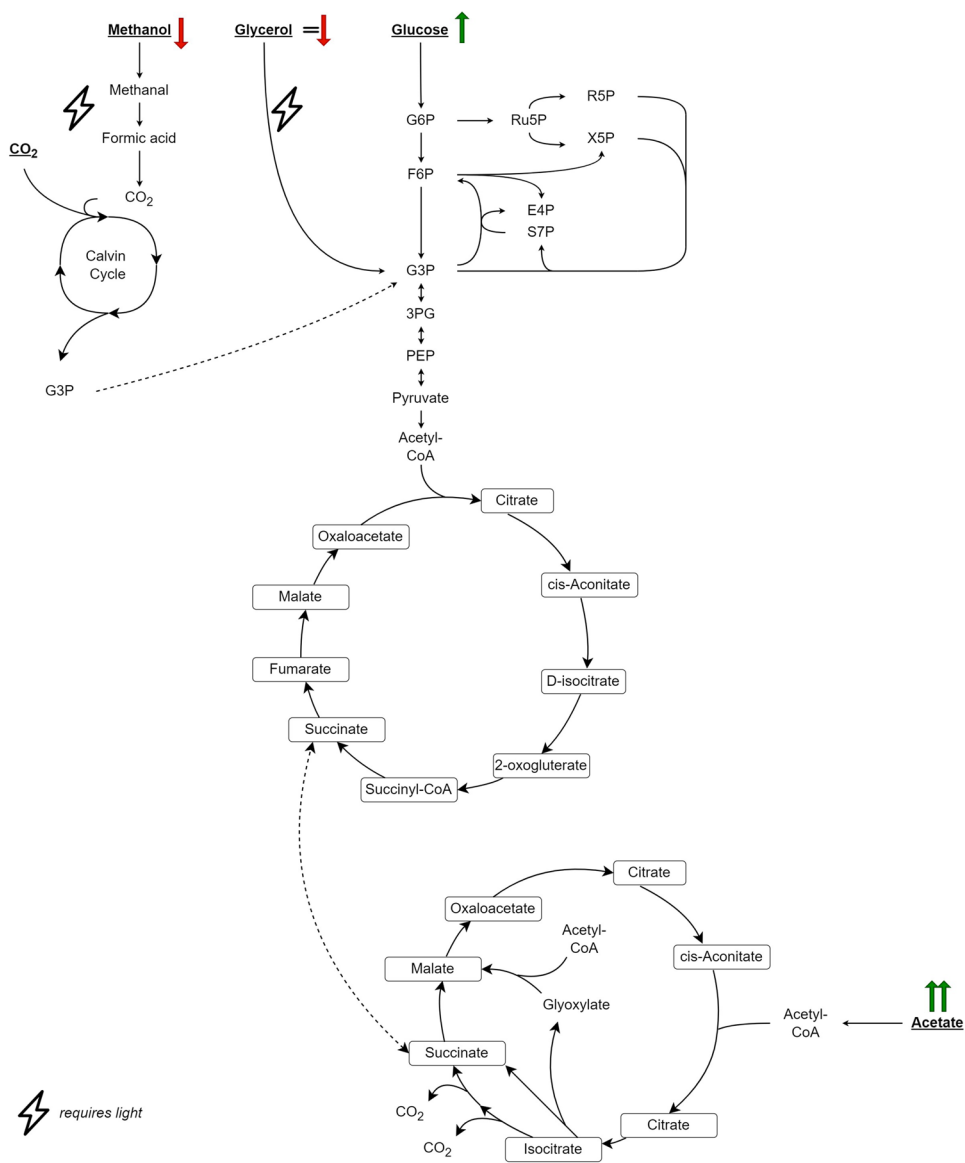
A comparison with other studies shows, that our findings fall in a similar range for mixotrophic growth on acetate and glucose (Table 3). While a clear discrepancy is found for mixotrophic growth on glycerol, which is discussed in more detail below. The slightly lower growth rates ranging from 0.57 to  $0.60 \text{ day}^{-1}$  for cultures grown on acetate can be attributed to the lower light intensity of  $20 \mu\text{mol photons m}^{-2} \text{s}^{-1}$ . The reported yield of 1.08 g biomass per g of acetate is almost double the highest yield observed in this study, however the higher efficiency in their study could again be connected to the lower light intensity (Kobayashi et al. 1992). Since a lower photosynthetically activity will result in a smaller  $\text{CO}_2$  fixation which could make the appearance of a more efficient conversion of acetate to biomass. Similarly, the slightly higher growth rates on glucose can be explained by the deployed illumination strategy of incremental increases from 60 to  $170 \mu\text{mol photons m}^{-2} \text{s}^{-1}$  (Oncel et al. 2011). Unfortunately, most studies did not report uptake rates or yields on substrate and no study was found in which methanol was used for mixotrophic growth of *H. lacustris*. The

differences of this study compared to previous studies remark the complexity of mixotrophic growth and that several simultaneous parameters play a significant role for the metabolism and thereby kinetics of *H. lacustris*.

Explaining the effect of different carbon sources on growth can be challenging as there are several phenomena involved, which can have a direct or indirect influence: (1) substrate concentration; (2) uptake mechanisms; (3) theoretical energy of the component; and (4) rate limiting reactions in the metabolic pathways (Fig. 3). Not all effects can be explained by the experiments performed in this study. However, hypotheses can be made based on further knowledge presented in the literature. The substrate concentration was below  $1.3 \text{ g L}^{-1}$  for all sources to identify limitations at low concentrations. Substrate inhibition was only observed for glycerol, but it cannot be ruled out that other carbon

sources become inhibitory at higher concentrations (Liang et al. 2009). Glucose and acetate require active transporters, whereas glycerol and methanol enter the cell through diffusion. However, glucose and acetate cultivations showed higher growth rates despite requiring more energy for the active uptake. The standard heat of combustion, which can be interpreted as the energy content per mole, of acetate, glucose, glycerol, and methanol is  $874, 2800, 1654$  and  $726 \text{ kJ mol}^{-1}$ , respectively (Engineering ToolBox 2017). This could explain why glucose yields higher growth rates than glycerol, despite their similarities in metabolic pathways. Nonetheless, acetate with the second lowest theoretical energy promoted the fastest growth. Therefore, metabolic pathways appear to be the most influential aspect in understanding the effect of the carbon source on mixotrophic growth. Acetate assimilation is the only substrate discussed

**Fig. 3** Schematic representation of the carbon cycle in *Haematococcus lacustris*. Arrows indicate the improvement (green-up) and reduction (red-down) in growth compared to photoautotrophic growth. G6P, glucose 6-phosphate; F6P, fructose 6-phosphate; 3PG, 3-phosphoglycerate; PEP, phosphoenolpyruvate; Ru5P, ribulose-5-phosphate; R5P, ribose 5-phosphate; X5P, Xylulose-5-phosphate; E4P, erythrose 4-phosphate; S7P, sedoheptulose-7-phosphate



here that does not share glyceraldehyde-3-phosphate (G3P) as an intermediate with photoautotrophic carbon fixation. This could indicate a rate-limiting step in the conversion of G3P to carbon skeletons and ATP, which would explain the strong synergistic effect observed under mixotrophic conditions with acetate (Table 4).

Although the glycerol concentration had a significant influence on the growth rate of *H. lacustris*, growth rates were similar to photoautotrophic growth rate. Significant inhibition was statistically (LSD,  $p < 0.05$ ) confirmed for glycerol concentrations above 30 mM C, while no increase in growth rate was observed at lower concentrations. Furthermore, the uptake and metabolization of glycerol could not be confirmed through ICS analysis. Contrarily, a few studies claim a positive effect of glycerol on the mixotrophic growth in *H. lacustris* (Andruleviciute et al. 2014; Azizi et al. 2019; Dechatiwongse and Choorit 2021). In addition, Azizi et al. (2019) and Dechatiwongse and Choorit (2021) showed that glycerol was consumed in their cultures and claimed a positive effect of glycerol on growth. However, the growth rates obtained in mixotrophic conditions with glycerol are not significantly different from the photoautotrophic control (ANOVA analysis,  $p < 0.05$ ). All studies in which glycerol contributed to higher growth rates were conducted at higher light intensities ranging from 60 to 250  $\mu\text{mol photons m}^{-2} \text{s}^{-1}$ , which could be the reason for the contradictory results. Since the first of three steps to metabolize glycerol to G3P is ATP dependent, an excess of energy provided by photosynthesis might be required. This hypothesis is further strengthened when considering the inability of *H. lacustris* to grow on glycerol without the presence of light (Dechatiwongse and Choorit 2021).

Higher growth and lipid production has been reported for various microalgae when grown in mixotrophic conditions with methanol (Choi et al. 2011; Plöhn et al. 2022). However, to our best knowledge, no studies have been conducted in which *H. lacustris* was exposed to methanol. Similar to other solvents, methanol can have toxic effects on microorganisms. This is mostly related to alterations in the cell membrane structure, hindering vital cell mechanisms (Weber and De Bont 1996). The inhibiting effect observed in this study when growing *H. lacustris* at methanol concentrations below 10 mM C could emerge from alterations in the cell wall and membrane. Whereas, at higher concentrations,

the methanol, could be converted to carbon dioxide (Kotzabasis et al. 1999). A positive effect compared to photoautotrophic growth was not observed at any concentration, indicating that the additional  $\text{CO}_2$  generated from the methanol does not improve growth significantly.

Among all experiments the growth on acetate displayed by far the highest growth rates with no significant effect seen by the acetate concentration. The small impact of concentration indicates that the uptake affinity of the monocarboxylic/proton transporter protein is high, which would enable efficient fed-batch systems at low concentrations of acetate. The additional knowledge of yields on acetate, which were presented here, and online or at-line monitoring of the biomass concentration would provide sufficient information to set up an efficient process where acetate remains at low concentrations below 0.1  $\text{g L}^{-1}$  while maintaining maximum growth. The effluent of anaerobic processes such as fermentation or anaerobic digestion is rich in acetate and can therefore be used to cultivate *H. lacustris* (M. Pan et al. 2021). Other available nutrients such as nitrogen and phosphorous increase the value of these waste streams, enabling a cost-effective solution to increase the productivity of natural astaxanthin production through *H. lacustris*.

## Light intensities

Mixotrophic growth was higher at any investigated light intensity and at the respective optimum the mixotrophic growth rate was more than 2.6 times higher than photoautotrophic growth. One could describe mixotrophic growth as the sum of photoautotrophic and heterotrophic growth (Wagner et al. 2016). However, even when accounting for heterotrophic growth, mixotrophic growth was 1.8 times higher than the sum of hetero- and photoautotrophic growth. Smith et al. (2015) observed a similar phenomenon in the freshwater microalgae *Micratinium inermum*. They investigated the gas exchange of dissolved inorganic carbon (DIC) and dissolved oxygen (DO) at mixotrophic conditions and concluded that there is a synergistic effect of DIC and DO formed by respiration and photosynthesis, respectively. Similarly, a synergistic effect of locally available DIC from the acetate metabolism and DO could improve growth in addition to the energy provided by additional organic carbon.

**Table 4** Overview of characteristics of the used carbon sources including theoretical energy, uptake and metabolism

Carbon source	Standard heat of combustion ( $\text{kJ mol}^{-1}$ )	Active transporter	Metabolic pathways involved
Glucose	2800	Yes	Glycolysis, Pentose phosphate pathway, TCA cycle
Methanol	726	No	Methanol oxidation, Formate metabolism
Glycerol	1654	No	Glycolysis, TCA cycle
Acetate	874	Yes	Glyoxylate cycle, TCA cycle



Our experiments clearly show a high sensitivity of green, vegetative *H. lacustris* cells toward light intensity. Therefore, when modeling the effect of light intensity on growth, the model must be able to describe photoinhibition. However, the light tolerance in the mixo- and photoautotrophic conditions was significantly different. According to the applied model, the optimum light intensity was 1.3 times higher at mixotrophic conditions compared to the photoautotrophic conditions. This implies a significantly higher tolerance for high light intensities at mixotrophic conditions, as observed in studies on astaxanthin induction (Wang et al. 2022). Wang et al. (2022) proposed a regulatory mechanism in response to high light stress for *H. lacustris*. This mechanism consists of three cellular responses: (1) an increase in the ratio of photosystem I and photosystem II; (2) enhanced astaxanthin accumulation; and (3) thickening of the cell wall. Our results suggest that some of these mechanisms are not

only crucial for cellular protection but might also result in stronger light being beneficial for growth under mixotrophic conditions. Adaptations in the photosystem and the cell wall will presumably not directly improve growth but rather be in place to maintain the cell. However, moderate accumulation of astaxanthin would improve light tolerance since astaxanthin can reduce the number of reactive oxygen species (ROS), which are a direct result of higher light intensities (Domonkos et al. 2013). To accumulate astaxanthin the cell enhances photorespiration, Embden-Meyerhof-Parnas (EMP) pathway and, the pentose phosphate pathway (PPP; (Yu et al. 2022b)). Resulting in G3P and glyoxylate accumulation of which the latter facilitates exogenous acetate assimilation (Fig. 4). Acetate supplies the cell directly with carbon required for astaxanthin synthesis, which represents a more efficient way compared to CO<sub>2</sub> fixation (Orosa et al. 2005). A similar effect was observed by Jeon et al. (2006),

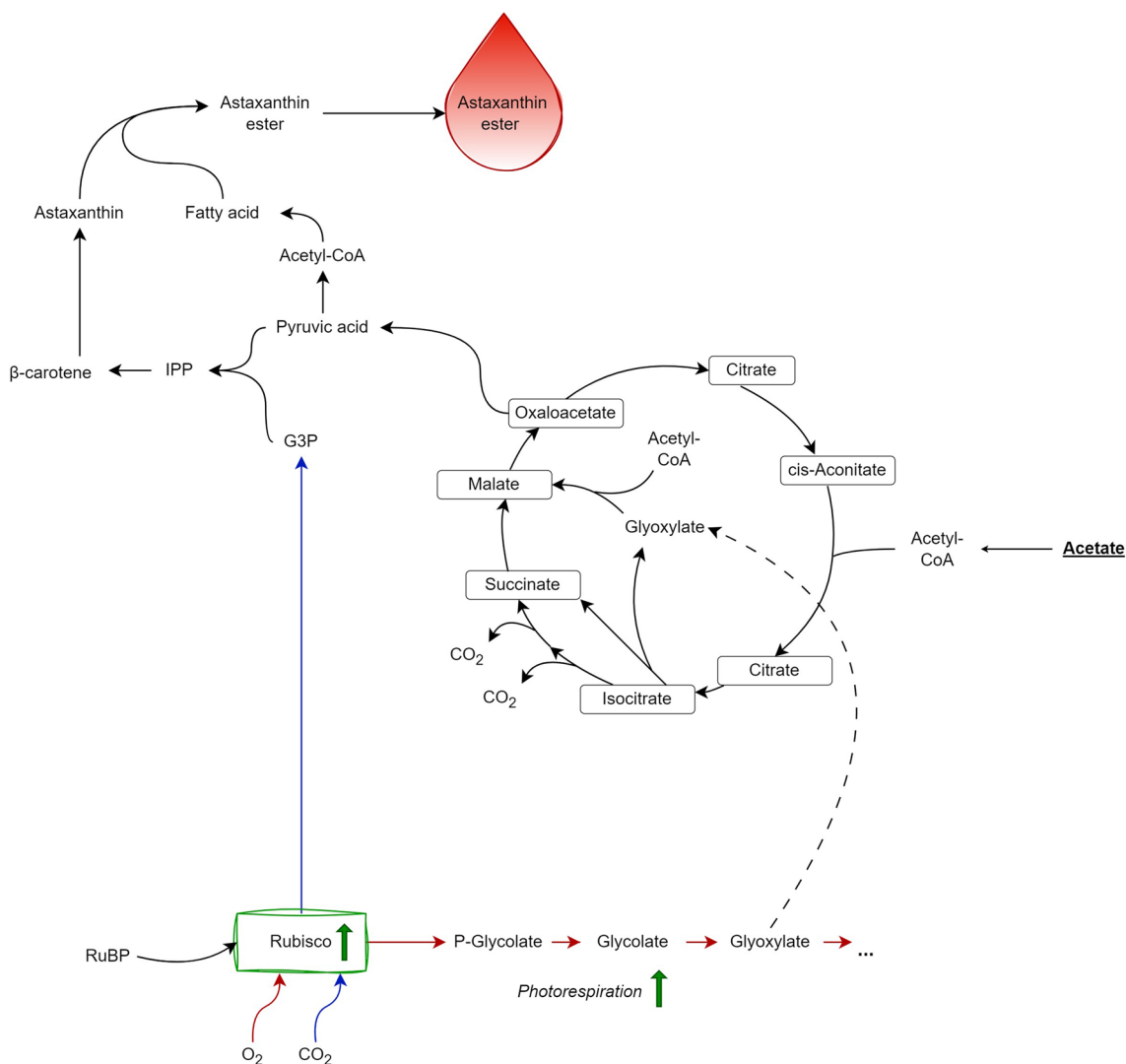


Fig. 4 Potential photo-protection mechanism under mixotrophic conditions. IPP, isopentenyl pyrophosphate; RuBP, ribulose-1,5-biphosphate

who reported positive effects on cell growth and the vegetative cell cycle during mixotrophic growth of *H. lacustris* with acetate.

This demonstrates that mixotrophic cultivation of *H. lacustris* not only constitutes a promising strategy to increase growth rates and cell densities but could also function for photoprotection. Outdoor cultivation systems (e.g. tubular photobioreactors) where the incident light intensity cannot be controlled could therefore benefit from a mixotrophic cultivation strategy.

Moreover, the compensation light intensity was predicted to be 1.5 times lower for mixotrophic conditions. Since *H. lacustris* can grow heterotrophically under dark conditions, a compensation light intensity does not exist for cultures supplemented with sodium acetate. However, in our experiments, heterotrophic growth was only possible when the cultures were aerated. Hence, even low light intensities, below the compensation light intensity of photoautotrophic growth, appear to positively influence mixotrophic growth.

### Challenges modelling mixotrophic, heterotrophic and photoautotrophic growth

Mathematical models enable efficient process design and control due to the ability to predict growth or other relevant characteristics based on operational parameters such as light intensity and nutrient concentration. In this study, we determined the growth kinetics of four carbon sources and the growth kinetics in respect to light in photoautotrophic and mixotrophic conditions. These experiments exposed two major challenges. Firstly, the description of mixotrophic growth of *H. lacustris* cannot be considered the sum of autotrophic and heterotrophic growth rates. Secondly, the availability of organic carbon directly influences parameters associated with the growth on light (e.g.,  $I_{\max}$ ,  $I_{\text{ph,c}}$ ). Several mathematical models describing mixotrophic growth of microalgae assume that mixotrophic growth can be described by the sum of heterotrophic and photoautotrophic growth (Adesanya et al. 2014; Wagner et al. 2016; Figueroa-Torres et al. 2017). Additionally, some studies also account for the availability of oxygen and carbon dioxide, respectively produced from photosynthesis and carbon oxidation, which could be an efficient way to implement the synergistic effects occurring at mixotrophic growth (Wagner et al. 2016; Manhaeghe et al. 2020). Nonetheless, none of these models account for interactions between kinetics for light intensity and the presence of organic carbon. *Haematococcus lacustris* is significantly more light-sensitive compared to other industrial-relevant microalgae such as *Chlorella vulgaris*, which may be a critical factor for commercial applications (Wu et al. 2020). Based on the outcomes of our study we conclude that considering  $O_2$  and  $CO_2$  concentration could be insufficient to simulate the synergistic effect observed in mixotrophic conditions for *H. lacustris*. Additional multiplier might

be required to depict the apparent synergistic effects. Furthermore, we propose to determine the light-dependent parameters separately under mixo- and photoautotrophic conditions.

### Conclusions

Acetate, glucose, and methanol can be utilized by *H. lacustris* in the presence of low light intensity, while glycerol uptake was not confirmed. Mixotrophic growth using glucose, methanol, and glycerol was dependent on the substrate concentration, whereas acetate concentration did not significantly influence the growth rate. The latter resulted in the biggest improvement in respect to growth compared to photoautotrophic conditions. Furthermore, mixotrophic conditions using acetate as an exogenous carbon source displayed growth in a wider range of light intensities than in photoautotrophic conditions. The maximum specific growth rate was found at significantly higher light intensities, which could be applied in closed outdoor systems to increase the light tolerance of *H. lacustris*. Finally, the detailed kinetic descriptions lay the foundation for a modelling framework which could be applied to carbon-rich waste streams.

**Supplementary Information** The online version contains supplementary material available at <https://doi.org/10.1007/s10811-024-03322-x>.

**Authors' contributions** LS: Conceptualisation, Methodology, Software, Validation, Formal analysis, Investigation, Data curation, Writing – Original Draft, Writing – Review&Editing, Visualisation. BVP: Conceptualisation, Supervision, Writing – Review&Editing. AT: Supervision, Writing – Review&Editing. IA: Supervision, Writing – Review&Editing, Project administration, Funding Acquisition. All authors contributed to the article and approved the submitted version.

**Funding** Open access funding provided by Technical University of Denmark. This research has received funding from the Digitalgaesation project within the European Union's Horizon 2020 research and innovation program under the Marie Skłodowska-Curie grant agreement No. 955520. Also, it was supported by Blue BioEconomy—2020 (BluBiochain) cofunded by Innovation Foundation Denmark (File number: 1036-00003B) and EU (ERA-NET BlueBio- no 31).

**Data availability** All data generated or analyzed during this study are included in this published article and the supporting information.

### Declarations

**Declaration of competing interest** The authors declare any potential financial or other interests that could be perceived to influence the outcomes of this research.

**Competing Interests** The authors declare no competing interests.

**Open Access** This article is licensed under a Creative Commons Attribution 4.0 International License, which permits use, sharing, adaptation, distribution and reproduction in any medium or format, as long as you give appropriate credit to the original author(s) and the source, provide a link to the Creative Commons licence, and indicate if changes were made. The images or other third party material in this article are included in the article's Creative Commons licence, unless indicated

otherwise in a credit line to the material. If material is not included in the article's Creative Commons licence and your intended use is not permitted by statutory regulation or exceeds the permitted use, you will need to obtain permission directly from the copyright holder. To view a copy of this licence, visit <http://creativecommons.org/licenses/by/4.0/>.

## References

- Abreu AP, Morais RC, Teixeira JA, Nunes J (2022) A comparison between microalgal autotrophic growth and metabolite accumulation with heterotrophic, mixotrophic and photoheterotrophic cultivation modes. *Renew Sust Energy Rev* 159:112247
- Adesanya VO, Davey MP, Scott SA, Smith AG (2014) Kinetic modelling of growth and storage molecule production in microalgae under mixotrophic and autotrophic conditions. *Bioresour Technol* 157:293–304
- Ambati RR, Moi PS, Ravi S, Aswathanarayana RG (2014) Astaxanthin: Sources, extraction, stability, biological activities and its commercial applications - A review. *Mar Drugs* 12:128–152
- Andrews JF (1968) A mathematical model for the continuous culture of microorganisms utilizing inhibitory substrates. *Biotechnol Bioeng* 10:707–723
- Andrulėvičiūtė V, Makarevičiūtė V, Skorupskaitė V, Gumbyte M (2014) Biomass and oil content of *Chlorella* sp., *Haematococcus* sp., *Nannochloris* sp. and *Scenedesmus* sp. under mixotrophic growth conditions in the presence of technical glycerol. *J Appl Phycol* 26:83–90
- APHA (1999) Standard methods for the examination of water and wastewater (20th ed.). American Public Health Association (APHA), Washington D.C.
- Azizi M, Hejazi MA, Hashemi M (2019) Supplementation with polyalcohols and sequential mixotrophy dilution photoinduction strategy boost the accumulation of astaxanthin by *Haematococcus pluvialis*. *Aquaculture* 511:734225
- Barbera E, Sforza E, Bertucco A (2015) Maximizing the production of *Scenedesmus obliquus* in photobioreactors under different irradiation regimes: experiments and modeling. *Bioprocess Biosyst Eng* 38:2177–2188
- Becker HM, Hirnet D, Fecher-Trost C, Sültemeyer D, Deitmer JW (2005) Transport activity of MCT1 expressed in *Xenopus* oocytes is increased by interaction with carbonic anhydrase. *J Biol Chem* 280:39882–39889
- Boyle NR, Morgan JA (2009) Flux balance analysis of primary metabolism in *Chlamydomonas reinhardtii*. *BMC Systems Biol* 3:4
- Choi WY, Oh SH, Seo YC, Kim GB, Kang DH, Lee SY, Jung KH, Cho JS, Ahn JH, Choi GP, Lee HY (2011) Effects of methanol on cell growth and lipid production from mixotrophic cultivation of *Chlorella* sp. *Biotechnol Bioproc Eng* 16:946–955
- Cooper GM, Hausman RE (2013) Transport of small molecules. In: *The cell: a molecular approach*, 6th edn. Sinauer Associates, Sunderland, pp 526–543
- Dechatiwongse P, Choerit W (2021) Mixotrophic growth of astaxanthin-rich alga *Haematococcus pluvialis* using refined crude glycerol as carbon substrate: Batch and fed-batch cultivations. *Walailak J Sci Technol* 18(2), 1–20
- Domínguez A, Pereira S, Otero A (2019) Does *Haematococcus pluvialis* need to sleep? *Algal Res* 44:101722
- Domonkos I, Kis M, Gombos Z, Ughy B (2013) Carotenoids, versatile components of oxygenic photosynthesis. *Progr Lipid Res* 52:539–561
- Droop MR (1974) Heterotrophy of carbon. In: Stewart WDP (ed) *Algal Physiology and Biochemistry*. Blackwell, Oxford, pp 530–559
- Engineering ToolBox (2017) Combustion heat. [https://www.engineeringtoolbox.com/standard-heat-of-combustion-energy-content-d\\_1987.html](https://www.engineeringtoolbox.com/standard-heat-of-combustion-energy-content-d_1987.html)
- Figuroa-Torres GM, Pittman JK, Theodoropoulos C (2017) Kinetic modelling of starch and lipid formation during mixotrophic, nutrient-limited microalgal growth. *Bioresour Technol* 241:868–878
- Haldane JBS (1930) *Enzymes*. Longmans, Green & Co., London
- Henry EC (2004) *Handbook of Microalgal Culture: Biotechnology and Applied Phycology*. *J Phycol* 40:1001–1002
- Ingram LO, Calder JA, van Baalen C, Plucker FE, Parker PL (1973) Role of reduced exogenous organic compounds in the physiology of the blue green bacteria (Algae): Photoheterotrophic growth of a “heterotrophic” blue green bacterium. *J Bacteriol* 114:695–700
- Jeon YC, Cho CW, Yun YS (2006) Combined effects of light intensity and acetate concentration on the growth of unicellular microalga *Haematococcus pluvialis*. *Enz Microb Technol* 39:490–495
- Kaplan D, Richmond AE, Dubinsky Z, Aaronson A (1986) Algal nutrition. In: Richmond A (ed) *Handbook of Microalgal Mass Culture*. CRC Press, Boca Raton, pp 147–198
- Kobayashi M, Kakizono T, Yamaguchi K, Nishio N, Nagai S (1992) Growth and astaxanthin formation of *Haematococcus pluvialis* in heterotrophic and mixotrophic conditions. *J Ferment Bioeng* 74:17–20
- Kotzabasis K, Hatziathanasiou A, Kentouri M (1999) Methanol as alternative carbon source for quicker efficient production of the microalgae. *1656:357–362*
- Li X, Wang X, Duan C, Yi S, Gao Z, Xiao C, Agathos SN, Wang G, Li J (2020) Biotechnological production of astaxanthin from the microalga *Haematococcus pluvialis*. *Biotechnol Adv* 43:107602
- Liang Y, Sarkany N, Cui Y (2009) Biomass and lipid productivities of *Chlorella vulgaris* under autotrophic, heterotrophic and mixotrophic growth conditions. *Biotech Lett* 31:1043–1049
- Lin Y, He Y, Meng Z, Yang S (2008) Anaerobic treatment of wastewater containing methanol in upflow anaerobic sludge bed (UASB) reactor. *Front Env Sci Eng in China* 2:241–246
- Manhaeghe D, Blomme T, Van Hulle SWH, Rousseau DPL (2020) Experimental assessment and mathematical modelling of the growth of *Chlorella vulgaris* under photoautotrophic, heterotrophic and mixotrophic conditions. *Water Res* 184:116152
- Maurya R, Zhu X, Valverde-Pérez B, Ravi Kiran B, General T, Sharma S, Kumar Sharma A, Thomsen M, Venkata Mohan S, Mohanty K, Angelidaki I (2022) Advances in microalgal research for valorization of industrial wastewater. *Bioresour Technol* 343:126128
- Mohamadnia S, Thygesen A, Ghofrani-Isfahani P, Monachese AP, Borja Valverde-Pérez, Angelidaki I (2023) Valorization of potato starch wastewater using anaerobic acidification coupled with *Chlorella sorokiniana* cultivation. *J Appl Phycol* 35:2645–2658
- Monod J (1949) The growth of bacterial cultures. *Annu Rev Microbiol* 3:371–394
- Neilson AH, Lewin RA (1974) The uptake and utilization of organic carbon by algae: an essay in comparative biochemistry. *Phycologia* 13:227–264
- Oncel SS, Imamoglu E, Gunerken E, Sukan FV (2011) Comparison of different cultivation modes and light intensities using mono-cultures and co-cultures of *Haematococcus pluvialis* and *Chlorella zofingiensis*. *J Chem Technol Biotechnol* 86:414–420
- Orosa M, Franqueira D, Cid A, Abalde J (2005) Analysis and enhancement of astaxanthin accumulation in *Haematococcus pluvialis*. *Bioresour Technol* 96:373–378
- Oslan SNH, Shoparwe NF, Yusoff AH, Rahim AA, Chang CS, Tan JS, Oslan SN, Arumugam K, Ariff AB, Sulaiman AZ, Mohamed MS (2021) A review on *Haematococcus pluvialis* bioprocess optimization of green and red stage culture conditions for the production of natural astaxanthin. *Biomolecules* 11:256
- Pan M, Zhu X, Pan G, Angelidaki I (2021) Integrated valorization system for simultaneous high strength organic wastewater treatment and astaxanthin production from *Haematococcus pluvialis*. *Bioresour Technol* 326:124761

- Pan XR, Wang YK, Li WW, Wang YS, Wang X, Cheng Y, Geng YK, Li CX, Lam PKS, Yu HQ (2017) Selective co-production of acetate and methane from wastewater during mesophilic anaerobic fermentation under acidic conditions. *Environ Sci: Water Res Technol* 3:720–725
- Perez-Garcia O, Escalante FME, de-Bashan LE, Bashan Y (2011) Heterotrophic cultures of microalgae: metabolism and potential products. *Water Res* 45:11–36
- Plöhn M, Scherer K, Stagge S, Jönsson LJ, Funk C (2022) Utilization of different carbon sources by Nordic microalgae grown under mixotrophic conditions. *Front Mar Sci* 9:830800
- Proietti Tocca G, Agostino V, Menin B, Tommasi T, Fino D, Di Caprio F (2024) Mixotrophic and heterotrophic growth of microalgae using acetate from different production processes. *Rev Env Sci Biotech* 23:93–132
- Ranga Rao A, Raghunath Reddy RL, Baskaran V, Sarada R, Ravishankar GA (2010) Characterization of microalgal carotenoids by mass spectrometry and their bioavailability and antioxidant properties elucidated in rat model. *J Ag Food Chem* 58:8553–8559
- Ruiz J, Olivieri G, De Vree J, Bosma R, Willems P, Reith JH, Eppink MHM, Kleinegriss DMM, Wijffels RH, Barbosa MJ (2016) Towards industrial products from microalgae. *Energy Environ Sci* 9:3036–3043
- Sauer N, Tanner W (1989) The hexose carrier from *Chlorella*. cDNA cloning of a eucaryotic H<sup>+</sup>-cotransporter. *FEBS Lett* 259:43–46
- Smith RT, Bangert K, Wilkinson SJ, Gilmour DJ (2015) Synergistic carbon metabolism in a fast growing mixotrophic freshwater microalgal species *Micractinium inermum*. *Biomass Bioenergy* 82:73–86
- Starr RC, Zeikus JA (1993) UTEX—The culture collection of algae at the University of Texas at Austin 1993 List of Cultures. *J Phycol* 29:1–106
- Steele JH (1962) Environmental control of photosynthesis in the sea. *Limnol Oceanogr* 7:137–150
- 't Lam GP, Vermeuë MH, Eppink MHM, Wijffels RH, van den Berg C (2018) Multi-product microalgae biorefineries: from concept towards reality. *Trends Biotech* 36:216–227
- Van Wagenen J, Holdt SL, De Francisci D, Valverde-Pérez B, Plósz BG, Angelidaki I (2014) Microplate-based method for high-throughput screening of microalgae growth potential. *Bioresour Technol* 169:566–572
- Vidotti ADS, Riaño-Pachón DM, Mattiello L, Giraldi LA, Winck FV, Franco TT (2020) Analysis of autotrophic, mixotrophic and heterotrophic phenotypes in the microalgae *Chlorella vulgaris* using time-resolved proteomics and transcriptomics approaches. *Algal Res* 51:102060
- Vigato F, Angelidaki I, Woodley JM, Alvarado-Morales M (2022) Dissolved CO<sub>2</sub> profile in bio-succinic acid production from sugars-rich industrial waste. *Biochem Eng J* 187:108602
- Wágner DS, Valverde-Pérez B, Sæbø M, Bregua de la Sotilla M, Van Wagenen J, Smets BF, Plósz BG (2016) Towards a consensus-based biokinetic model for green microalgae – The ASM-A. *Water Res* 103:485–499
- Wang B, Pan X, Wang F, Liu L, Jia J (2022) Photoprotective carbon redistribution in mixotrophic *Haematococcus pluvialis* under high light stress. *Bioresour Technol* 362:127761
- Weber FJ, De Bont JAM (1996) Adaptation mechanisms of microorganisms to the toxic effects of organic solvents on membranes. *Biochim Biophys Acta - Rev Biomembr* 1286:225–245
- Wu K, Ying K, Liu L, Zhou J, Cai Z (2020) High irradiance compensated with CO<sub>2</sub> enhances the efficiency of *Haematococcus lacustris* growth. *Biotechnol Rep* 26:e00444
- Yu BS, Lee SY, Sim SJ (2022a) Effective contamination control strategies facilitating axenic cultivation of *Haematococcus pluvialis*: Risks and challenges. *Bioresour Technol* 344:126289
- Yu W, Zhang L, Zhao J, Liu J (2022b) Enhancement of astaxanthin accumulation in *Haematococcus pluvialis* by exogenous oxaloacetate combined with nitrogen deficiency. *Bioresour Technol* 345:126484
- Zhang C, Liu J, Zhang L (2017) Cell cycles and proliferation patterns in *Haematococcus pluvialis*. *Chin J Oceanol Limnol* 35:1205–1211
- Zhang Z, Wang B, Hu Q, Sommerfeld M, Li Y, Han D (2016) A new paradigm for producing astaxanthin from the unicellular green alga *Haematococcus pluvialis*. *Biotechnol Bioeng* 113:2088–2099

**Publisher's Note** Springer Nature remains neutral with regard to jurisdictional claims in published maps and institutional affiliations.